UKAEA-CCFE-PR(20)22

M.S. Anastopoulos-Tzanis, B.D. Dudson, C.J. Ham,
C.C. Hegna, P.B. Snyder, H.R. Wilson

Non-Axisymmetric Equilibrium and Stability using the ELITE Stability Code

Non-Axisymmetric Equilibrium and Stability using the ELITE Stability Code

M.S. Anastopoulos-Tzanis, B.D. Dudson, C.J. Ham, C.C. Hegna,
P.B. Snyder, H.R. Wilson

This is a preprint of a paper submitted for publication in
Nuclear Fusion

Non-Axisymmetric Equilibrium and Stability using the ELITE Stability Code

M.S. Anastopoulos-Tzanis [1,2], B.D. Dudson [1], C.J. Ham [2], C.C. Hegna [3], P.B. Snyder [4], H.R. Wilson [1,2]

1) York Plasma Institute, Department of Physics, University of York, York, YO10 5DD, UK

2) Culham Centre for Fusion Energy, Abingdon, Oxon OX14 3DB, UK

3) Departments of Engineering Physics and Physics, University of Wisconsin-Madison, Madison, Wisconsin 53706, USA

4) General Atomics, San Diego, California 92186-5608, USA

October 2018

Abstract. A linear perturbation theory is used to model the MHD stability of tokamak equilibria under the application of external 3D magnetic perturbations [C.C. Hegna, *Physics of Plasmas* **21**:072502, 2014]. The symmetry breaking produces the coupling of toroidal n modes. We use ELITE [H.R. Wilson et al., *Physics of Plasmas* **9**:1277, 2002] to produce both a linearly perturbed non-axisymmetric equilibrium state as well as the linear axisymmetric modes, that are coupled for the stability analysis. The symmetry breaking produces coupling of modes with different toroidal mode number n and poloidal localisation of the non-axisymmetric peeling-ballooning mode is observed in comparison to the axisymmetric case.

1. Introduction

The efficient production of fusion power requires large pressure at the plasma core while retaining low pressure at the plasma edge, such that plasma facing components (PFCs) operate in an acceptable environment. Such pressure profiles are observed in high confinement mode (H-mode) plasmas. However, the establishment of a steep pressure gradient at the edge, so called pedestal region, together with large bootstrap driven edge current density is potentially destabilising for peeling-ballooning (PB) instabilities [1]. Those instabilities are manifested as edge localised modes (ELMs) and correspond to rapid bursts of particles and heat to PFCs, especially to the divertor of the reactor. For large tokamaks like ITER, those transients will result in heat fluxes that exceed the melting point of tungsten [2], the main material of the divertor tiles. Therefore, active ELM control methods are required to minimise potential damage of the reactor [3].

One method of ELM control that is widely applied to devices around the world and will be installed in ITER, uses external non-axisymmetric resonant magnetic perturbations (RMPs) produced from magnetic coils placed inside the tokamak vessel.

Experimental observations indicate two main operational states, one with ELM mitigation and the other with complete ELM suppression. In mitigation, a decreased energy loss per ELM ΔW_{ELM} leads to an increase of ELM frequency f_{ELM}. For ITER-like shape low density $n/n_{GW} \sim 0.3$, where $n_{GW} = I_p/\pi a^2$ is the Greenwald density limit, and low collisionality $\nu^* = \nu_{ei}\sqrt{m_e/k_B T_e}\epsilon^{-3/2}qR \sim 0.01$, complete suppression has only been observed at DIII-D [4] and recently in AUG [5], while for higher collisionality $\nu^* \sim 1$ KSTAR [6] has also achieved ELM suppression. The exact physics mechanism that allows this ELM free regime is still to be understood. In addition, ITER will operate in a high density $n/n_{GW} \sim 0.7$ low collisionality $\nu^* \sim 0.01$ regime such that extrapolation from current machines could be challenging in the absence of a rigorous physics basis.

In general, external 3D fields affect transport and MHD properties of the plasma. The resonant component of the field drives current structures at rational surfaces that can in turn lead to magnetic islands that greatly increase perpendicular transport [7],[8],[9]. As a result, the pressure gradient in the pedestal is relaxed and global stability boundaries are not exceeded. However, plasma flow that exists in the pedestal region can be strong enough that island structures could heal [10],[11]. In addition, the geometrical change of the equilibrium can affect MHD instabilities leading to potential modification of stability boundaries that can directly affect the onset of ELMs. Ideal infinite-n ballooning analysis reveals that the dominant effect of the applied 3D is to alter the local shear, which has significant consequences for local MHD stability [12],[13],[14]. However, for intermediate-n modes responsible for the occurrence of ELMs, a global 3D analysis is needed. Recent work on 3D stability has been performed [15],[16] but not yet applied to an ELM control scenario. To some extent, such an investigation has been performed by non-linear fluid codes and mode coupling was observed to be the key mechanism to achieve a suppressed operational regime [17].

This work focuses on the impact of toroidal symmetry breaking on the ideal MHD stability of the plasma. In a toroidally axisymmetric system the toroidal variation of the response is described by linearly decoupled discrete toroidal modes, i.e. toroidal mode number n, is a good quantum number and only poloidal coupling occurs. Considering an additional non-axisymmetric part of the equilibrium that is much smaller than the axisymmetric part, typically $\delta B/B \sim 10^{-4}$, together with approximately retained nested flux surfaces, linear perturbation theory can be employed to provide the required geometrical coupling of the axisymmetric modes. This coupling will result in energy transfer between neighbouring toroidal Fourier modes that can directly affect the evolution of instabilities. In this paper, we will explore this coupling mechanism.

2. Perturbative Ideal MHD

The above mentioned analysis was performed to first order in Ref.[18] and then to second order in Ref.[19]; this is required to capture perturbative non-axisymmetric effects.

Considering the force-balance equation,

$$-\omega_n^2\vec{\xi}_n = (\vec{F}+\delta\vec{F})\vec{\xi}_n \tag{1}$$

where ω_n^2 is the real eigenvalue of the system, the force operator can be separated into an axisymmetric part $\vec{F}$ and non-axisymmetric part $\delta\vec{F}$ part; provided $\vec{F} \gg \delta\vec{F}$, the non-axisymmetric force can be treated as a perturbation. The axisymmetric operator $\vec{F}$ is Hermitian and provides the equation for the unperturbed system which corresponds to the 0^{th} order equation,

$$-\omega_{n0}^2\vec{\xi}_{n0} = \vec{F}\vec{\xi}_{n0} \tag{2}$$

and a spectrum of real eigenvalues ω_{n0}^2 arises, provided that $(\vec{\xi}_{n0},\vec{\xi}_{m0}) = \delta_{nm}$, where $(a,b) = \int a^* b dV$. The solution $\vec{\xi}_n$ of the perturbed system can be approximated by a superposition of orthogonal eigenfunctions $\{\vec{\xi}_{n0},\vec{\xi}_{n1},\vec{\xi}_{n2},...\}$ and eigenvalues $\{\omega_{n0},\omega_{n1},\omega_{n2},...\}$ that correspond to solutions of the relevant ordered equation projected on the unperturbed sate $\vec{\xi}_{n0}$. The 1^{st} order equation,

$$-\omega_{n0}^2\vec{\xi}_{n1} - \omega_{n1}^2\vec{\xi}_{n0} = \vec{F}\vec{\xi}_{n1} + \delta\vec{F}\vec{\xi}_{n0} \tag{3}$$

gives a correction $-\omega_{n1}^2 = (\vec{\xi}_{n0},\delta\vec{F}\vec{\xi}_{n0}) = \delta V_{nn}$ due to axisymmetric changes of the plasma equilibrium. The 2^{nd} order equation,

$$-\omega_{n0}^2\vec{\xi}_{n2} - \omega_{n1}^2\vec{\xi}_{n1} - \omega_{n2}^2\vec{\xi}_{n0} = \vec{F}\vec{\xi}_{n2} + \delta\vec{F}\vec{\xi}_{n1} \tag{4}$$

is required for the case of non-axisymmetric RMP fields and results in a correction $-\omega_{n2}^2 = (\vec{\xi}_{n0},\delta\vec{F}\vec{\xi}_{n1})$. The structure of the perturbation $\vec{\xi}_{n1}$ is required and can be obtained considering Eqn.3. The orthogonal nature of a perturbation $(\vec{\xi}_{n0},\vec{\xi}_{n1}) = 0$ implies that it can be expressed as a series, summing over a basis of the unperturbed functions $\vec{\xi}_{n1} = \sum_{m\neq n} c_{nm}\vec{\xi}_{m0}$. Projecting Eqn.3 with respect to $\vec{\xi}_{m0}$ results in an expression for $c_{nm} = -\delta V_{mn}/(\omega_{n0}^2 - \omega_{m0}^2)$, where $\delta V_{mn} = (\vec{\xi}_{m0},\delta\vec{F}\vec{\xi}_{n0})$, such that the 1^{st} order correction in the displacement of a given mode is given by,

$$\vec{\xi}_{n1} = -\sum_{m\neq n}\frac{\delta V_{mn}}{\omega_{n0}^2 - \omega_{m0}^2}\vec{\xi}_{m0} \tag{5}$$

Substituting Eqn.5 into Eqn.4 and taking the inner product with $\vec{\xi}_{n0}$, provides a quantitative expression for the 2^{nd} order correction of the eigenvalue ω_{n2}^2,

$$\omega_{n2}^2 = \sum_{m\neq n}\frac{\|\delta V_{nm}\|^2}{\omega_{n0}^2 - \omega_{m0}^2} \tag{6}$$

It is interesting to note that for $\omega_{n0}^2 - \omega_{m0}^2 < 0$ the contribution is stabilising, while for $\omega_{n0}^2 - \omega_{m0}^2 > 0$ the contribution is destabilising. Therefore, for a spectrum $\omega_{n0}^2 > \omega_{m0}^2$ for $n > m$, coupling to higher modes has a stabilising contribution, while coupling to lower modes has a destabilising influence. Moreover, if the spectrum has a peak then this peak will always get more unstable.

Low-n ELITE [20],[21] is an axisymmetric MHD stability code that can very efficiently simulate the linear ideal plasma response from low to high n toroidal modes. ELITE solves the equation of motion for the normal plasma displacement functional that minimises the axisymmetric energy principle for an ideal incompressible plasma. In such a way, PB instabilities are captured and the ideal nature of the plasma retains nested flux surfaces, which is required for the perturbative stability analysis we adopt. Consequently, ELITE can be used to provide the radial axisymmetric basis eigenfunctions and (neglecting inertia) the 3D part of the plasma equilibrium, assuming the RMP mode is stable. We aim to use ELITE for both the equilibrium (plasma response) calculation and for the stability calculation since the code is optimised for the intermediate-to-high toroidal mode numbers that interest us. This is the first stage of a project to develop a tool which can optimise plasma response and ELM stability together.

3. Application to RMPs

The calculation of the non-axisymmetric part of the equilibrium requires an initial axisymmetric equilibrium that is stable to low-n toroidal modes, to be driven by RMP fields. We examine such an equilibrium here and the plasma profiles and axisymmetric PB stability analysis are illustrated in Fig.1. The external RMP field is based on a hypothetical even n=3 magnetic perturbation that is fixed and resonant at the plasma surface. The coordinate system used is based on the original axisymmetric equilibrium state.

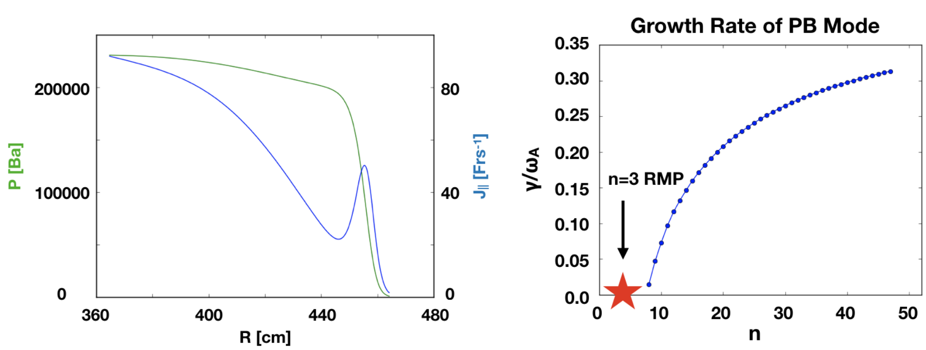

(a) (b)

Figure 1: Equilibrium radial plasma profiles for a) the plasma pressure and current density as well as b) the PB growth rate normalised to the Alfven frequency illustrating a stable equilibrium for low-n perturbations.

The plasma response is characterised by a kink-like displacement normal to the flux surfaces $\vec{\xi} \cdot \hat{n} \sim \delta B/B$ away from the rational surfaces. The normal displacement is strongly peaked around rational surfaces leading to large local response. The mode structure and the poloidal cross-section reconstruction of the normal displacement are depicted in Fig.2. The 3D magnetic equilibrium part can be calculated using $\vec{\xi}_\perp$ the plasma displacement perpendicular to the magnetic field. ELITE provides the normal displacement and through minimisation of the potential energy the binormal components

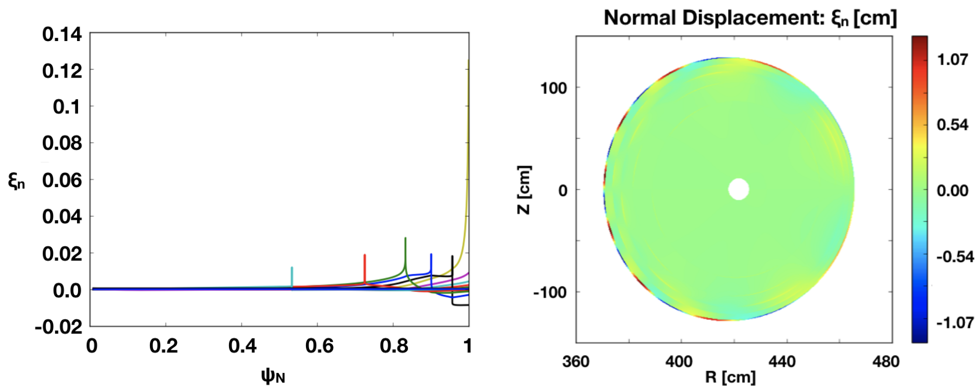

(a) (b)

Figure 2: a) Mode structure and b) poloidal cross-section reconstruction of the normal displacement $\vec{\xi} \cdot \hat{n}$ as reconstructed from ELITE output data for an even $n = 3$ RMP case.

can be obtained. The normal component of the field is imperfectly screened due to poloidal coupling in toroidal geometry, but individual modes are still screened at the corresponding rational surfaces so that island formation is prohibited in this ideal MHD model. This fact on its own shows that the existence of the plasma strongly modifies the external field in various ways. The normal field and its poloidal mode structure are illustrated in Fig.3.

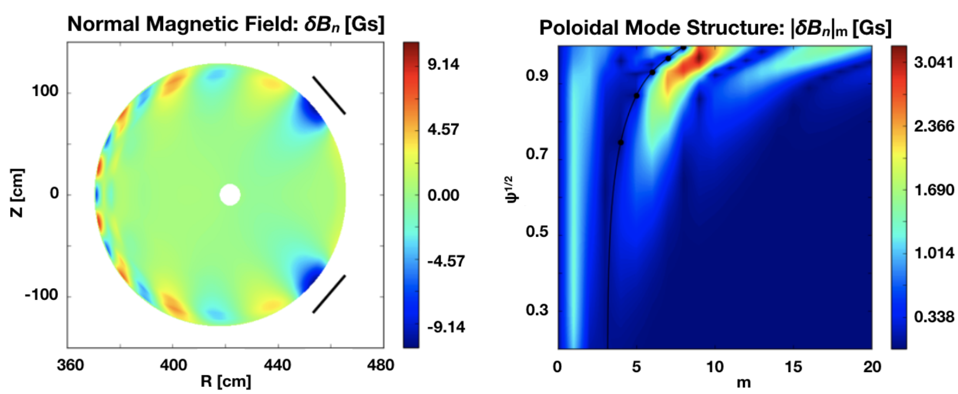

(a) (b)

Figure 3: Normal component of a) magnetic field and b) poloidal mode structure in a straight field-line angle as reconstructed from ELITE output data for an even n=3 RMP. The straight black lines indicate the position of the magnetic coils.

Fig.4 illustrates the parallel current density created around rational surfaces [22], which has two contributions. One contribution corresponds to the existence of Pfirsch-Schluter current density due to incompressibility and non-vanishing pressure gradient. The second contribution also arises from current incompressibility and for nested

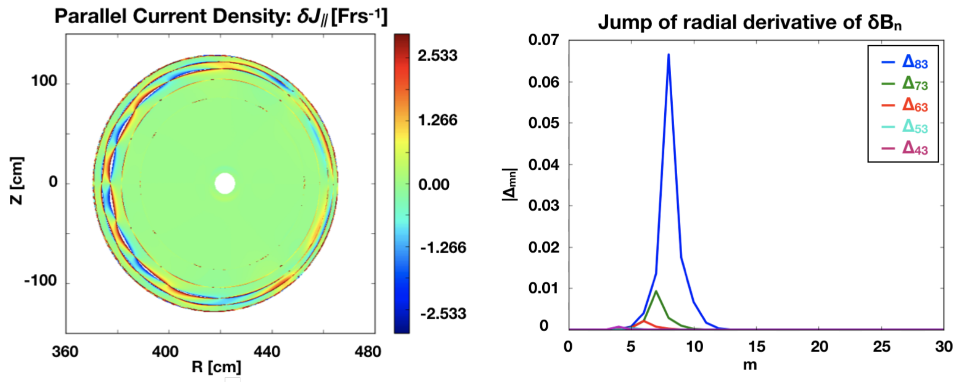

(a) (b)

Figure 4: a) Pfirsch-Schluter δJ_{PS} and b) Δ_{mn} factor of δ-like δJ_δ components of non-axisymmetric equilibrium parallel current density as reconstructed from ELITE.

flux surfaces corresponds to δ-like current layers. The calculation of those layers is numerically subtle but can be analytically quantified from the jump of the first derivative of the normal magnetic field Δ_{mn} according to Ref.[23].

The final perturbed equilibrium quantity needed for the coupling is the pressure gradient $\nabla\delta P$, calculated using the linearised pressure δP. The non-axisymmetric pressure profile is shown in Fig.5a. To verify the equilibrium obtained with ELITE, the non-linear code BOUT++ is used to perform a similar simulation. Both codes produced similar linear equilibrium states, with ELITE being more able to resolve sharp features around the rational surfaces due to much finer resolution. The comparison for the 3D equilibrium pressure is illustrated in Fig.5b.

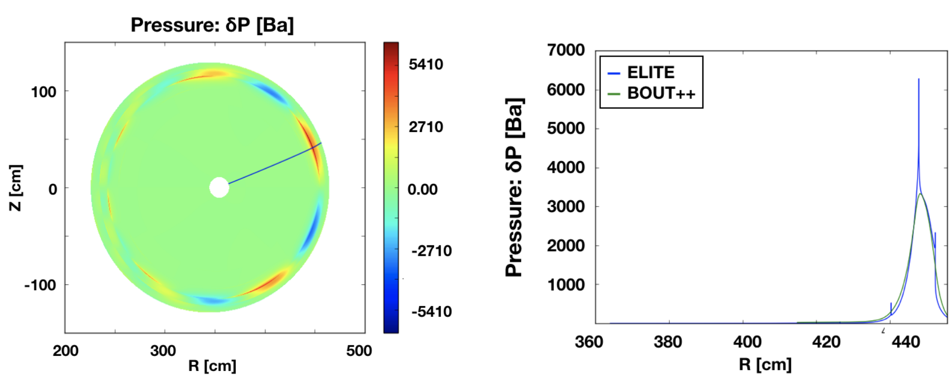

(a) (b)

Figure 5: a) Non-axisymmetric equilibrium plasma pressure δP as reconstructed from ELITE output data, b) from BOUT++ and a comparison between the two codes for fixed poloidal angle.

The coupling coefficients V_{nk} can be calculated using the above 3D equilibrium quantities $(\delta\vec{B}, \delta\vec{J}, \delta\vec{P})$ and axisymmetric toroidal modes $\{\vec{\xi}_{n0}\}$. It is observed that above a certain external field amplitude the impact of mode coupling is significant and that the dependence is non-linear with respect to the applied field strength. Fig.6a shows the strong stabilising influence of the 3D modification to the equilibrium geometry, due to stronger coupling with higher n toroidal modes, as discussed above. The reconstruction of the 3D normal displacement eigenmode of the instability results in a localised mode structure with respect to the poloidal location, due to the interplay of different axisymmetric modes. This 3D feature has been observed experimentally and reproduced successfully be infinite-n ballooning analysis [24]. A comparison between the mode structure of the axisymmetric and non-axisymmetric mode is illustrated in Fig.6b and Fig.6c.

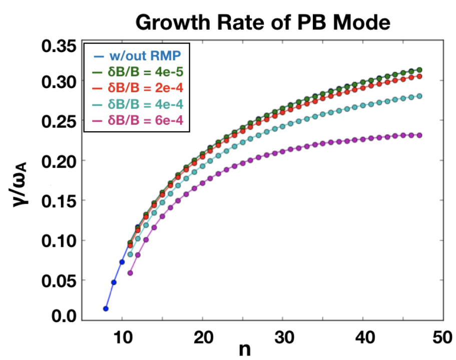

(a)

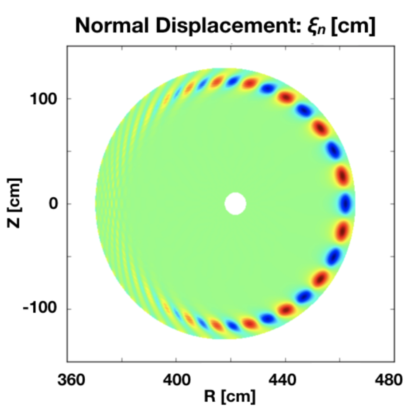

(b)

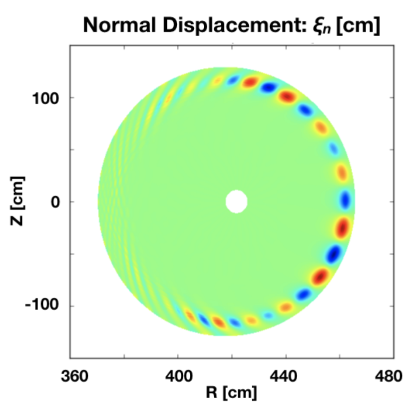

(c)

Figure 6: a) Perturbative 3D Peeling-Ballooning stability under the influence of varying amplitude external even n=3 RMP coil configuration $\delta B/B$ as reconstructed from ELITE output data. Normal plasma displacement $\vec{\xi} \cdot \hat{n}$ for a $n = 12$ b) axisymmetric and c) non-axisymmetric PB mode.

Finally, with respect to the plasma stability similar observations have been made using the non-linear code JOREK [17],[25],[26]. According to those simulations, a stochastic region at the plasma edge leads to degradation of the pedestal and a mitigated ELM state was observed. Although, ELM suppression was only obtained when mode coupling was enabled, provided the external field was above a certain threshold for mode coupling to become effective enough.

4. Conclusion

To summarise, applied RMP fields that break the axisymmetric nature of tokamak plasmas, are widely used to actively control ELMs. The 3D plasma stability can be studied in a perturbative way, as long as the full 3D equilibrium and the axisymmetric toroidal modes are known. The stability code ELITE provide both the axisymmetric toroidal eigenmodes required for the toroidal coupling and also the 3D part of the equilibrium. This was obtained by inserting a fixed boundary condition to represent an external field. Screening current density is captured, but has not been observed to have a strong impact on MHD stability. Nevertheless, the 3D equilibrium profiles and the geometrical mode coupling had a significant stabilising impact to MHD modes above a certain phenomenological threshold for the amplitude of the applied field. This is a consequence of stronger coupling to the higher n sideband of the axisymmetric system, which is more unstable for ballooning. For cases where the kink mode further destabilises intermediate n modes, the creation of a peak in the spectrum will lead to the opposite trend. Our results are consistent with non-linear fluid simulations and could provide further insight regarding the dominant physics mechanism that allows an ELM free operational state necessary for the advanced operation of ITER.

Acknowledgements

This work has been carried out within the framework of the EUROfusion Consortium and has received funding from the Euratom research and training programme 2014-2018 under grant agreement No 633053 and from the RCUK Energy Programme [grant number EP/P012450/1]. This research is supported in part by the U. S. Department of Energy (DOE) Office of Fusion Energy Sciences under grant no. DE-FG02-86ER53218.

References

[1] J.W. Connor et al., *Physics of Plasmas* **5:2687**, 1998
[2] R.A. Pitts et al., *Journal of Nuclear Materials* **438:48**, 2013
[3] A. Loarte et al., *Nuclear Fusion* **54:033007**, 2014
[4] T.E. Evans et al., *Nuclear Fusion* **48:024002**, 2008
[5] W.A. Suttrop et al., *Nuclear Fusion* **58:096031**, 2018
[6] Y. M. Jeon et al., *Physical Review Letter* **109:035004**, 2012
[7] R. Fitzpatrick, *Nuclear Fusion* **33:7**, 1993
[8] R.D. Hazeltine et al., *Physics Review Letter* **37:102**, 1976
[9] I. Joseph et al., *Nuclear Fusion* **48:045009**, 2008
[10] Y.Q. Liu et al., *Nuclear Fusion* **51:083002**, 2011
[11] M. Becoulet et al., *Nuclear Fusion* **52:054003**, 2012
[12] T.B. Cote et al., "Helically localised ballooning instabilities in three-dimensional tokamak Pedestals", *Nuclear Fusion* **submitted**, 2018
[13] T.M. Bird et al., *Nuclear Fusion* **53:013004**, 2013

[14] C.J. Ham et al., *Physics of Plasmas* **21:102501**, 2014
[15] E. Strumberger et al., *Nuclear Physics* **57:016032**, 2017
[16] T. Weyens et al., *Physics of Plasmas* **21:042507** 2014
[17] F. Orain et al., *Plasma Phys. Controlled Fusion* **57:014020**, 2015
[18] P. Helander et al., *Physics of Plasmas* **20:062504**, 2013
[19] C.C. Hegna, *Physics of Plasmas* **21:072502**, 2014
[20] H.R. Wilson et al., *Physics of Plasmas* **9:1277**, 2002
[21] A.E.L. Lunniss, *University of York* **PhD Thesis**, 2016
[22] P. Helander, *Reports on Progress in Physics* **77:087001**, 2014
[23] J.K. Park et al., *Physical Review Letter* **99:195003**, 2007
[24] M. Willensdorfer et al., *Physical Review Letter* **119:085002**, 2017
[25] F. Orain et al., *26th IAEA Fusion Energy Conference*, 2016
[26] F. Orain et al., *44th EPS Conference on Plasma Physics*, 2017